



Molecular Crystals and Liquid Crystals

Publication details, including instructions for authors and subscription information:

<http://www.tandfonline.com/loi/gmcl20>

Dynamic Properties of Polymer Stabilised Pi-Cells

P. D. Brimicombe^a, S. J. Elston^a & E. P. Raynes^a

^a Department of Engineering Science, University of Oxford, Oxford, United Kingdom

Version of record first published: 22 Sep 2010

To cite this article: P. D. Brimicombe, S. J. Elston & E. P. Raynes (2007): Dynamic Properties of Polymer Stabilised Pi-Cells, *Molecular Crystals and Liquid Crystals*, 476:1, 165/[411]-179/[425]

To link to this article: <http://dx.doi.org/10.1080/15421400701739089>

PLEASE SCROLL DOWN FOR ARTICLE

Full terms and conditions of use: <http://www.tandfonline.com/page/terms-and-conditions>

This article may be used for research, teaching, and private study purposes. Any substantial or systematic reproduction, redistribution, reselling, loan, sub-licensing, systematic supply, or distribution in any form to anyone is expressly forbidden.

The publisher does not give any warranty express or implied or make any representation that the contents will be complete or accurate or up to date. The accuracy of any instructions, formulae, and drug doses should be independently verified with primary sources. The publisher shall not be liable for any loss, actions, claims, proceedings, demand, or costs or damages

whatsoever or howsoever caused arising directly or indirectly in connection with or arising out of the use of this material.

Dynamic Properties of Polymer Stabilised Pi-Cells

P. D. Brimicombe

S. J. Elston

E. P. Raynes

Department of Engineering Science, University of Oxford, Oxford,
United Kingdom

The influence of the polymer network on the dynamic switching behaviour of polymer-stabilised pi-cell devices is investigated in detail. The stabilisation technique is shown experimentally to increase the relaxation and switch-on times of the device when small concentrations of polymer are used. Modelling of the device indicates that this is due to the polymer network suppressing the fluid flow during switching. A comparison between a conventional pi-cell and a polymer-stabilised device with the same switchable range of transmission indicates that addition of the polymer network increases the relaxation time by 1.7 times.

Keywords: fast-switching liquid crystal devices; pi-cell; polymer-stabilised liquid crystal device; reactive mesogen

INTRODUCTION

The pi-cell [1] or optically compensated bend (OCB) mode is widely regarded as the fastest switching nematic liquid crystal device technology. One of the primary drawbacks of the pi-cell is the fact that the V state must be nucleated before the device can be used. This nucleation can be unpredictable and unreliable. Use of polymer networks to stabilise the V state has been demonstrated [2], but only the static properties of such devices have been investigated in detail. The influence of the polymer stabilisation on the static and dynamic performance of pi-cell devices is investigated here.

The authors would like to thank the COMIT Faraday Partnership, the EPSRC and Merck UK for funding the project and Merck UK for supplying materials and devices.

Address correspondence to P. D. Brimicombe, Department of Engineering Science, University of Oxford, Parks road, Oxford, OX1 3PJ, United Kingdom. E-mail: paul.brimicombe@eng.ox.ac.uk

Pi-cells use untwisted nematic devices with splayed pretilts as shown in Figure 1. If the applied voltage is below $V_{th}(H-V)$, the H states are the long-term stable states. Above $V_{th}(H-V)$, the V state or bend state used for pi-cell operation becomes energetically favourable. This state is not topologically similar to the H states, however, and so must form via nucleation which typically takes some seconds to complete. If the applied voltage is allowed to fall below $V_{th}(H-V)$ the H states begin to nucleate into the pixel area once more.

Polymer stabilisation of the V state was first demonstrated by Kim and Chien [2]. A small concentration (< 10 wt%) of reactive mesogen (polymerisable liquid crystal material) is dissolved in the liquid crystal host along with a small amount of photoinitiator. The V state is nucleated by applying a voltage above $V_{th}(H-V)$. While a voltage above $V_{th}(H-V)$ is applied, the device is exposed to ultra-violet light and the reactive mesogen polymerises, forming a sparse polymer network that stabilises the V state.

In this work a mixture of reactive mesogen RM257 (Merck) and 5 wt% of photoinitiator Irgacure 907 (Ciba) has been dissolved in concentrations of between 1 wt% and 5 wt% into liquid crystal host ZLI 1132 (Merck). These mixtures were capillary filled into devices with a quoted pretilt of $1-2^\circ$ and thickness of $5\mu\text{m}$. Curing was carried out using a UV light source with a wavelength of 350 nm and an intensity of $\sim 30\text{ W/m}^2$ for 15 minutes to ensure full polymerisation.

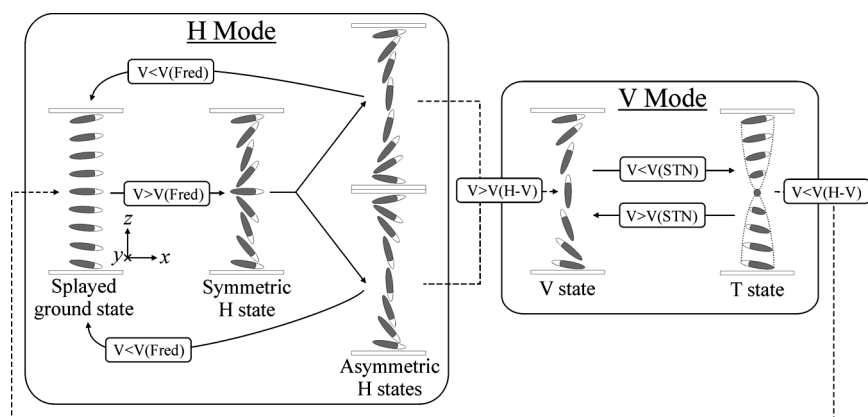


FIGURE 1 The states that form in nematic devices with splayed pretilts. The H and STN modes are not topologically similar, and so the transition from one to the other must occur through nucleation. The symmetric H state only forms transiently when a voltage is applied suddenly to the splayed ground state.

Previous work has indicated that low applied voltages during curing produce the best static response of the polymer stabilised device [2], and so a voltage just above $V_{th}(H-V)$ has been used here (3 Vrms). It was found that reactive mesogen concentrations of 1 wt% and below were not sufficient to stabilise the V state.

INFLUENCE OF THE APPLIED WAVEFORM DURING CURING

Although the rms of the applied waveform during curing has been investigated [2], the influence of the precise waveform used has not been reported previously. With a 2 wt% concentration of reactive mesogen and using a 3 Vrms square wave during curing, a granular texture is produced, similar to those seen in reference [2]. The right hand photomicrograph in Figure 2 shows this texture with the rubbing direction parallel to one of the crossed polarisers, and clearly the polymer network has produced polarisation scattering, making the device appear grey.

Diffusion during the curing process causes aggregates of the polymer to form, resulting in the granular texture seen when high frequency waveforms are used. If a 3 Vrms low frequency (e.g. 50 Hz) sine wave is used during curing, a much smoother texture is produced, reducing the polarisation scattering of the polymer network. The production of a more evenly distributed polymer network under these conditions is probably due to the flow in the device. When a square wave is applied to a liquid crystal device, the director orientation does not change during each cycle once equilibrium has been reached, since the dielectric torque is proportional to the square of the electric field. If a sine wave is used, however, the torque varies during each cycle and if the frequency used is low enough ($<1\text{ kHz}$), there is time for the

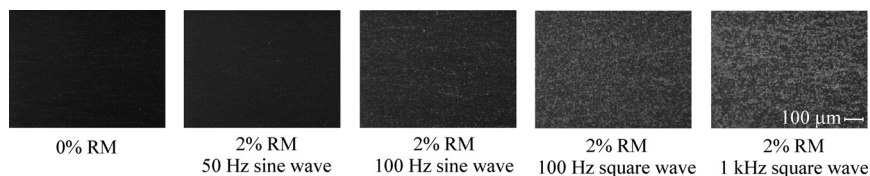


FIGURE 2 The influence of varying the waveform used to retain the V state whilst curing. When square waves are applied (right), a coarse texture is produced, with much polarisation scattering of the incident light. Using low frequency sine waves, the texture becomes smooth, and there is less polarisation scattering, which will lead to a higher quality dark state. The rms voltage of the waveforms used is constant at 3 Vrms.

liquid crystal to respond, and there are director fluctuations within each cycle. These fluctuations induce a flow in the device, which inhibits the diffusion of the reactive mesogens, preventing large polymer aggregates from forming. When concentrations of reactive mesogen above 2 wt% are used, the texture appears progressively more uniform, but lower frequency sine wave curing voltages still induce smoother textures. The devices discussed in the remainder of this paper were all cured whilst applying a 3 Vrms 50 Hz sine wave.

ADJUSTMENT FOR VARIATIONS IN DEVICE THICKNESS

A major problem when attempting to identify the influence of the polymer concentration on the device performance is variations in thickness between the different devices used. Thickness variations will alter the static and dynamic properties of the device significantly, and will severely limit the accuracy of the experiment. Once the device has been filled with the reactive mesogen and liquid crystal mixture, exposure to ambient light is not sufficient to polymerise the reactive mesogen because of the UV absorption of the glass substrates. This allows the light transmission through each device for a range of applied voltages to be measured before curing.

The light transmission through a birefringent slab between crossed polarisers with the optic axis at 45° to the polarisers is given by

$$\frac{I}{I_0} = \sin^2 \left(\frac{\pi \Delta n_{\text{eff}} d}{\lambda} \right), \quad (1)$$

where Δn_{eff} is the birefringence of the slab, d is the slab thickness and λ is the wavelength of the incident light. The retardation $\pi \Delta n_{\text{eff}} d / \lambda$ is then linear with the device thickness. Using Equation 1, the retardation of each device as a function of applied voltage can be found from the pre-cure light transmission measurements. These curves are then scaled linearly to make the curves coincident, since the only significant difference between the samples will be the variation in thickness. These linear scaling factors can then be used to adjust the data taken after curing in order to eliminate the influence of thickness variations on the results.

STATIC RETARDATION-VOLTAGE CURVES

Figure 3(a) shows the scaled pre-cure retardation of pi-cells filled with various concentrations of reactive mesogen as a function of the applied voltage (the data are scaled to the 2 wt% reactive mesogen device).

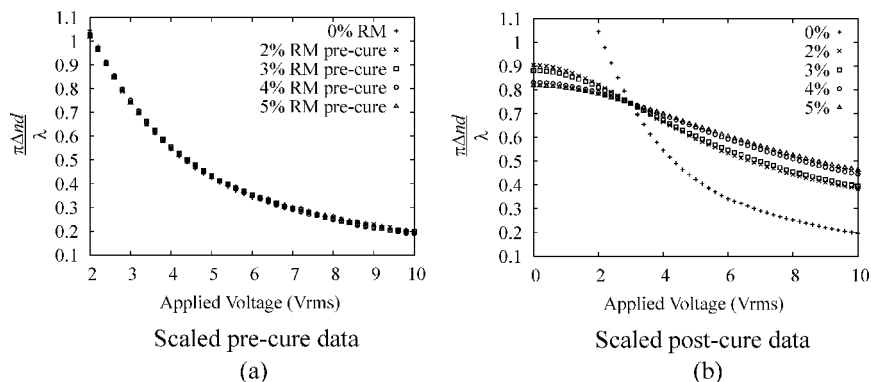


FIGURE 3 (a) Scaled pre-cure retardation against voltage characteristics of the different devices. The very good agreement between the devices shows that thickness variations have been adjusted for correctly. (b) The scaled post-cure electro-optic characteristics of the polymer stabilised devices. The retardation at the curing voltage (3 Vrms) is the same for all the devices.

The V state is nucleated in each device by applying a voltage above $V_{th}(H-V)$ prior to the measurements being taken. The thickness variation between the different devices is found to be less than 10%. The very good agreement between the datasets shown in Figure 3(a) indicates that the addition of the small percentage of reactive mesogen only has a small effect on the material properties of the liquid crystal host.

Figure 3(b) shows the post-cure retardation against voltage characteristics of the polymer-stabilised pi-cells. The same scaling factors have been used here as in Figure 3(a). The retardation at the curing voltage (3 Vrms) remains constant as the reactive mesogen concentration is increased. If a device were filled with 100% reactive mesogen, the retardation would remain constant at the curing voltage value after polymerisation regardless of the applied voltage. As the concentration of reactive mesogen is increased, this limit is progressively approached, leading to a smaller switchable range of retardation over a given voltage range. From static considerations alone, the lowest concentration of reactive mesogen possible should be used to retain a large switchable range of retardation.

MODELLING THE STATIC DEVICE RESPONSE

The behaviour of the polymer stabilised pi-cell can be modelled by adding an extra term [3] to the Frank elastic energy density of the

liquid crystal [4]:

$$w_d = \frac{1}{2} \left[K_{11} (\nabla \cdot \hat{n})^2 + K_{22} (\hat{n} \cdot \nabla \times \hat{n})^2 + K_{33} (\hat{n} \times \nabla \times \hat{n})^2 - K_a (\hat{n} \cdot \hat{p})^2 \right], \quad (2)$$

where \hat{n} is the liquid crystal director, K_{11} , K_{22} and K_{33} are the elastic constants associated with splay, twist and bend respectively, \hat{p} is the director profile of the polymer network and K_a is an *influence parameter* that defines the strength of the interaction between the polymer network and the bulk liquid crystal. This model assumes that the polymer network is rigid and remains identical to the director distribution at the voltage applied during curing. In addition, the optical activity of the polymer network has been ignored since the reactive mesogen concentrations used here are so small. The dielectric energy density, $-1/2\mathbf{D} \cdot \mathbf{E}$, is added to Eq. (2), and the director profile is found using a one dimensional Euler-Lagrange routine to minimise the total free energy of the device (variations within the plane of the device are ignored since the pixel is large when compared to the device thickness).

Figure 4 shows the results of modelling the retardation-voltage characteristics of the 0wt% and 2wt% reactive mesogen devices.

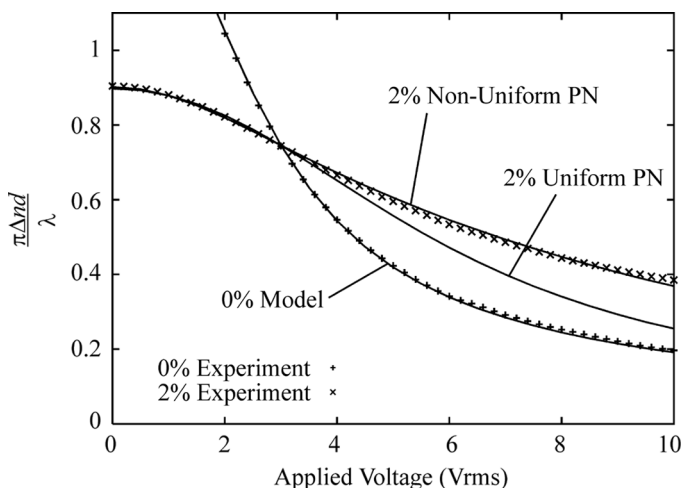


FIGURE 4 Modelling of the static retardation-voltage characteristic of the polymer stabilised pi-cell. The fit to the experimental data is very good in the conventional pi-cell. Using a uniform polymer network, the fit is good for low voltages, but not for higher voltages. Using a non-uniform polymer network, the fit is significantly improved.

The fit to the non-stabilised pi-cell data is very good, indicating that the physical parameters used in simulation (those from the manufacturer's datasheet) are valid. If K_a is kept constant across the device thickness, a good fit for the 2 wt% device is found for $K_a = 100 \text{ Nm}^{-2}$, but only at low voltage. Since the host liquid crystal material used here (ZLI-1132) is moderately absorbing in the UV, it is reasonable to assume that the polymer network is more dense near the surfaces than in the bulk (the UV exposure was from both sides simultaneously). Non-uniformities of this kind have been observed previously [5].

By allowing K_a to vary through the device thickness ($K_a = K_a(z)$), a much better fit is can be obtained. In order to minimise the fitting parameters, a polynomial distribution of the form

$$K_a(z) = A(z - 0.5)^B \quad (3)$$

was used initially (A and B are fitting parameters). This function produces very high values of the influence parameter at the surfaces, causing the simulation to become unstable. Use of a cosine function of the form

$$K_a(z) = A \cos^B(\pi z/d) \quad (4)$$

instead produces a similar influence parameter distribution in the bulk of the device, but a much reduced value near the surfaces, while still requiring only two fitting parameters. Figure 4 shows the results using $A = 1700$ and $B = 18$ and the fit to the experimental data is much improved, but the trend at high voltages is still not quite correct. This discrepancy may be because the polymer network is not rigid, and flexes at higher voltages. While it is possible to model this effect, it leads to many new unknown parameters and derivation of the equations becomes complex because an arbitrary polymer network distribution is required in this case.

DYNAMIC COMPARISON WITH A CONVENTIONAL PI-CELL OF IDENTICAL THICKNESS

The thickness dependence of the switching time of conventional pi-cells is $\tau \propto d^2$. If the properties of the polymer stabilised devices are assumed to retain this thickness dependence, then the switching times of the devices should be scaled by the square of the scaling factors used in Figure 3. In order to compare the switching times of the polymer stabilised devices with those of a pi-cell of the same thickness, the switching must be between an addressing voltage and just above

$V_{th}(H-V)$. If the voltage falls below $V_{th}(H-V)$ at any time, there is nucleation of the H states in the non-stabilised device.

The scaled relaxation times to the 90% level of the polymer stabilised devices and a conventional pi-cell switching between a range of addressing voltages and 3 Vrms are shown in Figure 5. Using small concentrations of reactive mesogen causes an increase in the relaxation time. As the polymer concentration is increased further, however, the relaxation time is reduced, and by 4 wt% the polymer stabilised device is faster than the conventional pi-cell of the same thickness.

The scaled switch-on times to the 10% level for the same devices are shown in Figure 6. The polymer stabilised devices have consistently longer switch-on times than the conventional pi-cell across the whole range of reactive mesogen concentration tested. As the concentration is varied there are changes to the switch-on behaviour, but these are subtle when compared to the variation in the relaxation times.

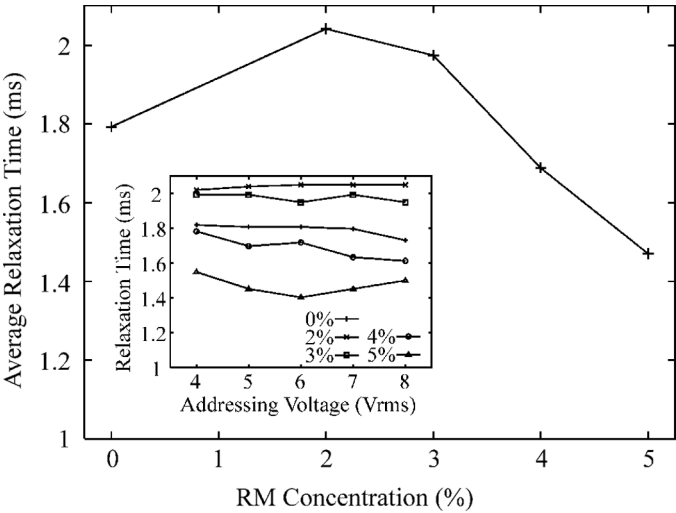


FIGURE 5 Comparison of the relaxation times to the 90% level between an addressing voltage and 3 Vrms of the polymer stabilised devices and a conventional pi-cell of the same thickness. Small concentrations of reactive mesogen increase the relaxation time, whereas larger concentrations decrease it. The relaxation time remains approximately constant across the range of addressing voltages used. The data have been scaled to eliminate any thickness variations between the samples.

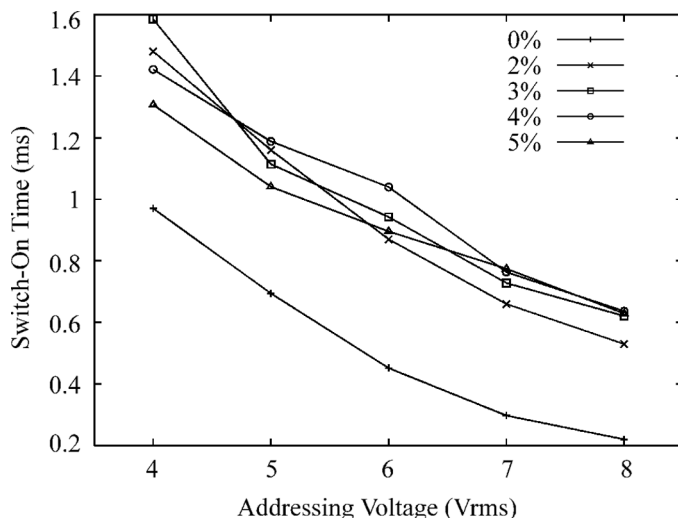


FIGURE 6 Comparison of the switch-on time to the 10% level of the polymer stabilised devices and a conventional pi-cell of the same thickness between 3 Vrms and an addressing voltage. The addition of the polymer network increases the switch-on time of the device. The data have been scaled to eliminate any thickness variations between the samples.

DYNAMIC MODELLING OF POLYMER STABILISED PI-CELLS

The rigid polymer network model from Eq. (2) can be used to simulate the dynamics of the polymer stabilised devices. The dynamic modelling technique uses Eriksen-Leslie-Parodi theory [6–8] with the van Doorn/Berreman approximation [9,10] except with the inclusion of the influence parameter shown in Eq. (2). The numerical solution method is outlined in reference [11], and the influenced parameters used were those found by fitting the static data (see Fig. 4). The simulated switching behaviour of the conventional pi-cell and the 2wt% polymer stabilised pi-cell ignoring flow is shown in Figure 7. The polymer network has little influence on the switch-on time, but does significantly alter the relaxation behaviour. In both the uniform and non-uniform polymer network cases the relaxation time is smaller than that of the conventional pi-cell. This is because the polymer network term in Eq. (2) adds to the elastic restoring torque in simulation. Experimentally, however, the relaxation and switch-on times of the 2 wt% polymer device are slower than those of the conventional pi-cell (see Fig. 5).

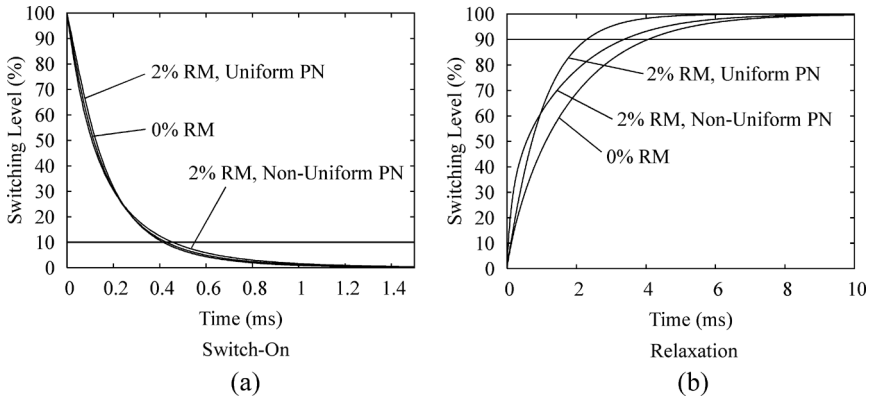


FIGURE 7 Simulated switch-on (a) and relaxation (b) curves of polymer stabilised and conventional pi-cells switching between 3 Vrms and 8 Vrms ignoring flow of the liquid crystal. The addition of the polymer network only has a small influence on the switch-on time, and leads to decreased relaxation times in both the uniform and non-uniform polymer network cases. This is not the experimentally observed behaviour (see Figs. 5 and 6).

It has been demonstrated that the shear flow during switching significantly reduces both the switch-on and relaxation times of conventional pi-cells [12]. The presence of the polymer network in the polymer stabilised devices may inhibit the shear flow of the liquid

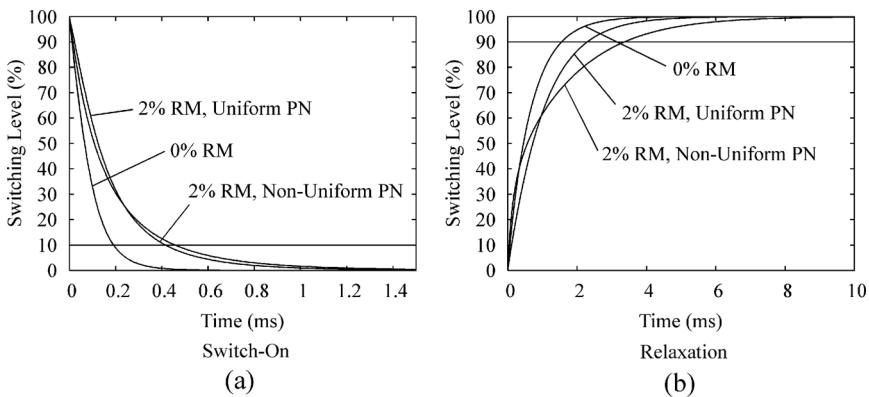


FIGURE 8 Simulated switch-on (a) and relaxation (b) curves of polymer stabilised and conventional pi-cells switching between 3 Vrms and 8 Vrms including flow of the liquid crystal in the conventional pi-cell only. The flow accelerates the switching of the conventional pi-cell, leading to faster switching times in both switch-on and relaxation.

crystal, and thus increase the switching times. Figure 8 shows a simulated comparison between a conventional pi-cell including fluid flow and the polymer stabilised pi-cells with flow effects suppressed completely. The switch-on time of the conventional pi-cell is now faster than that of the polymer stabilised devices, as is seen experimentally. In addition, the relaxation times to the 90% level of the polymer stabilised devices are slower than those of the conventional pi-cell for both the uniform and non-uniform polymer networks. The increase in switching times observed experimentally may also be due to dynamic flexing of the polymer network, but as described above, simulation of this effect introduces many unknown parameters.

SWITCHING OF THE POLYMER STABILISED PI-CELLS

Since the V state is now stable with no applied voltage, the polymer stabilised pi-cells can be switched between 0 Vrms and the addressing voltage, allowing operation over a greater range of retardation. The relaxation times of these devices under this addressing scheme are shown in Figure 9. Once again, increasing the reactive mesogen concentration decreases the relaxation time, and the relaxation times

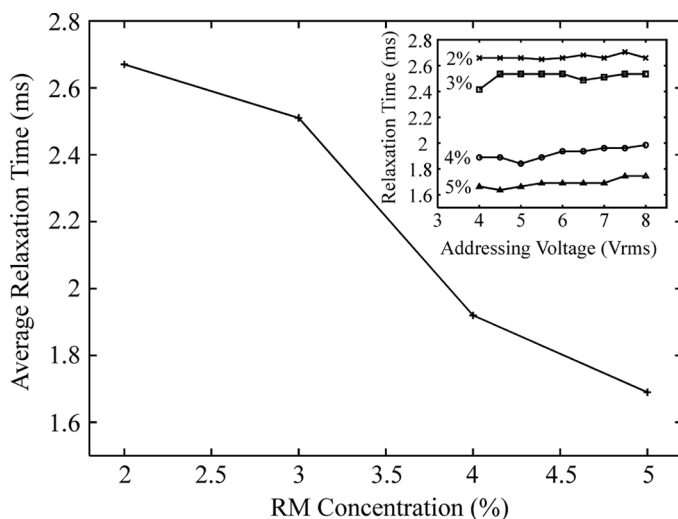


FIGURE 9 Experimental relaxation times of the polymer stabilised pi-cells from an addressing voltage to zero volts. The relaxation times are approximately independent of the addressing voltage, and follow the same trends as those shown in Figure 5. The data have been scaled to eliminate any thickness variations between the samples.

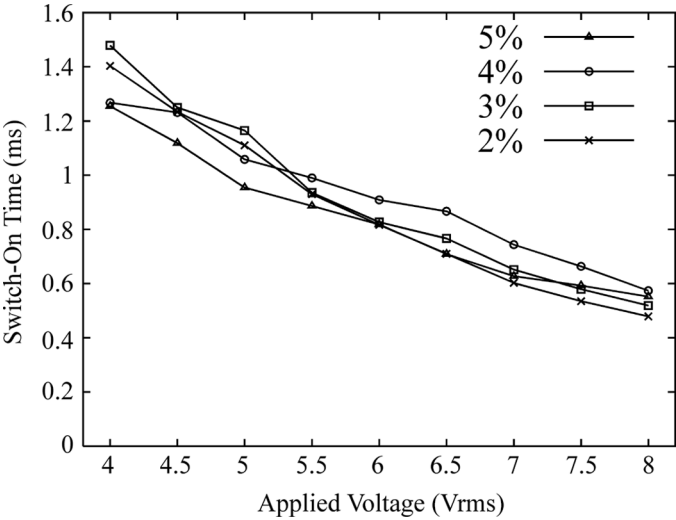


FIGURE 10 Experimental switch-on times of the polymer stabilised pi-cells from zero volts to an addressing voltage. As in the switching from 3 Vrms (Fig. 6), there is no clear trend as the reactive mesogen concentration is increased. The data have been scaled to eliminate any thickness variations between the samples.

are approximately independent of the addressing voltage. The relaxation times are consistently slower than those between the addressing voltage and 3 Vrms (see Fig. 5).

The switch-on times from 0 Vrms to an addressing voltage are shown in Figure 10. The switching times are similar to those obtained by switching from 3 Vrms to the addressing voltage (see Fig. 6). As the concentration of reactive mesogen is increased, there are subtle changes in the switch-on times, but no clear trend can be observed.

PREDICTION OF REAL DEVICE BEHAVIOUR

In real displays, the optical properties of a liquid crystal device must be optimised for the particular application. It is important, therefore, to compare devices that are capable of switching over the same transmission range. The highest voltage that can be applied to the device in a display is limited by the TFT array used. Typically, the highest voltage that a TFT can be operated at reliably is 8 Vrms. Any residual retardation of the pi-cell at this high voltage limit must be compensated using a retarder in order to produce a true dark state. This

compensation then also reduces the retardation at the lowest applied voltage (just above $V_{th}(H-V)$ for the conventional pi-cell and 0 Vrms for the polymer stabilised devices). In order to compare like-for-like devices, the range of switchable retardation after compensation should be the same for both devices. Using the static data shown in Figure 3, the thickness change required to meet this condition for each polymer stabilised device can be found. For example, the 2 wt% polymer device must be 1.07 times thicker than a conventional pi-cell to produce the same switchable retardation range after compensation.

Increasing the device thickness will also increase the relaxation time of the devices. Assuming that $\tau \propto d^2$, the experimentally obtained switching times are scaled in order to compare the switching times of like-for-like devices. The result of this scaling is shown in Figure 11, and as the reactive mesogen concentration is increased, the like-for-like relaxation time also increases. With higher reactive mesogen concentrations, the retardation against voltage characteristic becomes more shallow. A thicker device is therefore required to produce the same switchable retardation over a fixed voltage range. This increase in thickness slows the switching, and this dominates any improvement

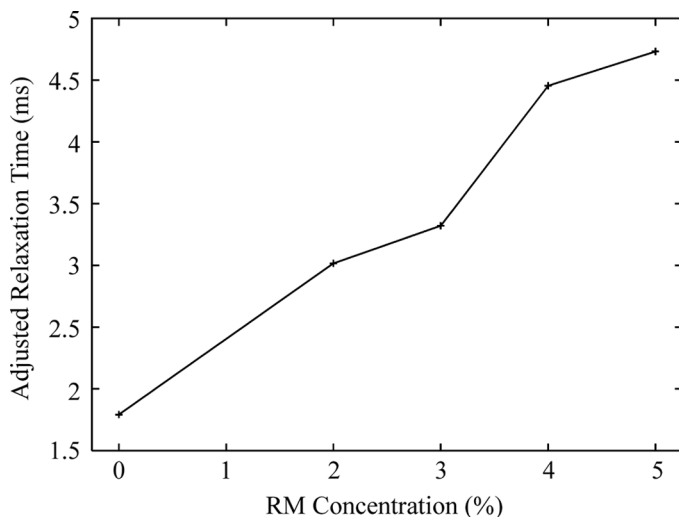


FIGURE 11 Like-for-like device switching time comparison. All devices switch over the same range of retardation. Any improvement in switching time observed in the higher reactive mesogen concentration devices (see Fig. 9) is cancelled out by the increase in thickness required to produce the same switchable range of retardation.

in the raw switching times achieved by using higher concentrations of reactive mesogen (see Figure 9). The optimum reactive mesogen concentration is therefore the lowest that still stabilises the V state. The relaxation time to the 90% level of the conventional pi-cell is 1.8 ms, whilst that of the equivalent 2 wt% reactive mesogen device is 3.0 ms.

CONCLUSIONS

The dynamic influence of the polymer network in polymer stabilised pi-cells has been investigated in detail. The use of low frequency sine waves to retain the V state during curing has been shown to produce less polymer aggregation, and thus less polarisation scattering. By taking the transmission against voltage characteristic of each device before curing, any thickness variations between the devices can be eliminated from the experiment. After curing, the retardation at the curing voltage is constant, regardless of the reactive mesogen concentration used. Static modelling of the device indicates that the polymer network is not uniform across the device thickness, and it is likely that the network flexes when higher voltages are applied. Use of low reactive mesogen concentrations has been shown to increase the relaxation time, and the presence of the polymer network increases the switch-on time, regardless of the reactive mesogen concentration. Dynamic modelling of the network indicates that this may well be because the polymer network is suppressing the fluid flow within the device. A like-for-like comparison between a conventional pi-cell and polymer stabilised pi-cells, indicates that the lowest possible polymer concentration should be used, and with the materials and devices used here, this corresponds to a reactive mesogen concentration of 2 wt%. Using this concentration, the relaxation time of the polymer stabilised device is increased by 1.7 times when compared to that of a conventional pi-cell capable of switching over the same range of retardation when the high voltage limit is 8 Vrms.

REFERENCES

- [1] Bos, P. J. & Koehler/Beran, K. R. (1984). *Mol. Cryst. Liq. Cryst.*, 113, 329.
- [2] Kim, S. H. & Chien, L. C. (2004). *Jpn. J. Appl. Phys.*, 43, 7643.
- [3] Li, J., Anderson, J. E., Hoke, C. D., Nose, T., & Bos, P. J. (1996). *Jpn. J. Appl. Phys.*, 35, L1342.
- [4] Frank, F. C. (1958). *Discuss. Faraday Soc.*, 25, 19.
- [5] Dessaud, N. & Raynes, E. P. (2002). *Liq. Cryst.*, 29, 391.
- [6] Eriksen, J. L. (1961). *Trans. Soc. Rheol.*, 5, 23.
- [7] Leslie, F. M. (1968). *Arch. Ration. Mech. Anal.*, 28, 265.

- [8] Parodi, O. (1970). *J. Physique*, 31, 581.
- [9] van Doorn, C. Z. (1975). *J. Appl. Phys.*, 46, 3738.
- [10] Berreman, D. W. (1975). *J. Appl. Phys.*, 46, 3746.
- [11] Brimicombe, P. D. & Raynes, E. P. (2005). *Liq. Cryst.*, 32, 1273.
- [12] Walton, H. G. & Towler, M. J. (2000). *Liq. Cryst.*, 27, 1329.